

J. Synchrotron Rad. (1999). **6**, 725–727

XAFS and XRD studies on local and long-range structures of mechanically alloyed $\text{Al}_x\text{Ti}_{1-x}$ solid solutions

Cui'e WEN^{a,b}, Kazuo YASUE^b, Shiqiang WEI^c, Tiandou HU^d and Hiroyuki OYANAGI^c

^a Dept. of Mater. Sci. and Eng., Beijing University of Aeronautics and Astronautics, Beijing, 100083, P.R.China.

^b Materials Processing Dept., National Industrial Research Institute of Nagoya, 1-1 Hirate-cho, Kita-ku, Nagoya 462-8510, Japan.

^c Electrotechnical Laboratory, 1-1-4 Umezono, Tsukuba, Ibaraki 305, Japan.

^d Beijing Synchrotron Radiation Facility, Beijing 100039, P.R. China.

E-mail: wen@nirin.go.jp

Local and long-range structures of mechanically alloyed $\text{Al}_x\text{Ti}_{1-x}$ alloys milled for 360 ks have been studied by XAFS and XRD. The XAFS results clearly show that there are similar radial distribution functions for $\text{Al}_{0.10}\text{Ti}_{0.90}$ and $\text{Al}_{0.50}\text{Ti}_{0.50}$ alloys. The Ti-Ti coordination number is 10.0 and 8.5 for $\text{Al}_{0.10}\text{Ti}_{0.90}$ and $\text{Al}_{0.50}\text{Ti}_{0.50}$ alloys, respectively. The Ti atoms in the $\text{Al}_{0.50}\text{Ti}_{0.50}$ alloy favor to be coordinated by Ti atoms in the first shell. The XRD results suggest that after milled for 360 ks the $\text{Al}_x\text{Ti}_{1-x}$ alloys form mixed phases of amorphous state and hcp $\text{Ti}(\text{Al})_{ss}$ solid solution for $x=0.10$ and 0.50 , and a single phase of fcc $\text{Al}(\text{Ti})_{ss}$ solid solution for $x=0.75$. The XRD result is in good agreement with that from XAFS. We propose that the mechanical alloying with a low power can drive the first nearest neighbor coordination around Ti atoms to produce a large defect, and extend $\text{Al}_x\text{Ti}_{1-x}$ amorphous alloy range to a lower Al concentration $x=0.10$.

Keyword: XAFS; $\text{Al}_x\text{Ti}_{1-x}$; mechanical alloying

1. Introduction

Titanium aluminides have been considered as very promising materials for potential applications in the aerospace industry (Kim *et al.*, 1992; Fleischer *et al.*, 1989) due to their attractive properties, such as high melting point, low density, high specific strength and modules, as well as odd oxidation and creep resistance. However, It is difficult to prepare the $\text{Al}_x\text{Ti}_{1-x}$ alloys by conventional metallurgy or rapid solidification techniques (Gerasimov *et al.*, 1996). Recently, mechanical alloying (MA) has attracted much attention for producing $\text{Al}_x\text{Ti}_{1-x}$ alloys. Gerasimov *et al.* (1991) have reported that the MA can drive $\text{Al}_{0.50}\text{Ti}_{0.50}$ to form hcp Al-Ti α_2 phase. In contrast, Park *et al.* (1992) and suryanarayana *et al.* (1990) have found that mixtures of α_2 and γ phases or amorphous alloy can be obtained for $\text{Al}_{0.50}\text{Ti}_{0.50}$, depending on the milling conditions. In addition, Burgio *et al.* (1990) has noted that amorphous alloys can be formed by MA for the composition $\text{Al}_x\text{Ti}_{1-x}$ with $x=0.2-0.5$. Nevertheless, Guo *et al.* (1992) and Saji *et al.* (1992) have considered that impurities of oxygen and nitrogen play an important role in the MA process forming a fcc Al_3Ti metastable phase. There are many contradiction conclusions obtained by different investigators. In

order to understand the nature of the MA $\text{Al}_x\text{Ti}_{1-x}$ alloys, it is essential to study the structural change of the $\text{Al}_x\text{Ti}_{1-x}$ system during the milling process.

In this paper, the combination of x-ray absorption fine structure (XAFS) and x-ray diffraction (XRD) have been performed to determine the local and long-range structures around Ti atoms in $\text{Al}_x\text{Ti}_{1-x}$ alloys during the ball milling process. We aimed at studying the local structure change around Ti atoms influenced by initial mixture composition for the $\text{Al}_x\text{Ti}_{1-x}$ system, then further investigate the MA mechanism of $\text{Al}_x\text{Ti}_{1-x}$ alloy.

2. Experimental

Elemental Al (reagent purity, 150 μm) and Ti (reagent purity, 50 μm) powders were mixed to the desired composition. The MA was performed in a planetary ball milling with a rotation speed of about 170 r/min, using hardened Cr steel vial under an argon atmosphere of 66 kPa. Several composition $\text{Al}_x\text{Ti}_{1-x}$ mixtures were milled for 360 ks.

Ti K-edge x-ray absorption spectra were measured at the XAFS station of 4W1B beamline of Beijing Synchrotron Radiation Facility. The electron beam energy was 2.2 GeV and the maximum stored currents is 70 mA. A fixed-exit Si(111) flat double crystals were used as monochromator. The x-ray harmonics were minimized by detuning the two flat Si(111) crystal monochromator to about 70% of the maximum incident light intensity. Data were collected in a transmission mode using ion chambers filled by N_2 gas at room temperature. The x-ray diffraction measurements of $\text{Al}_x\text{Ti}_{1-x}$ alloys were performed with a Philips PW-1800 x-ray diffractometer.

3. Results

The XRD patterns of several composition $\text{Al}_x\text{Ti}_{1-x}$ powders milled for 360 ks are shown in figure 1. It can be observed that

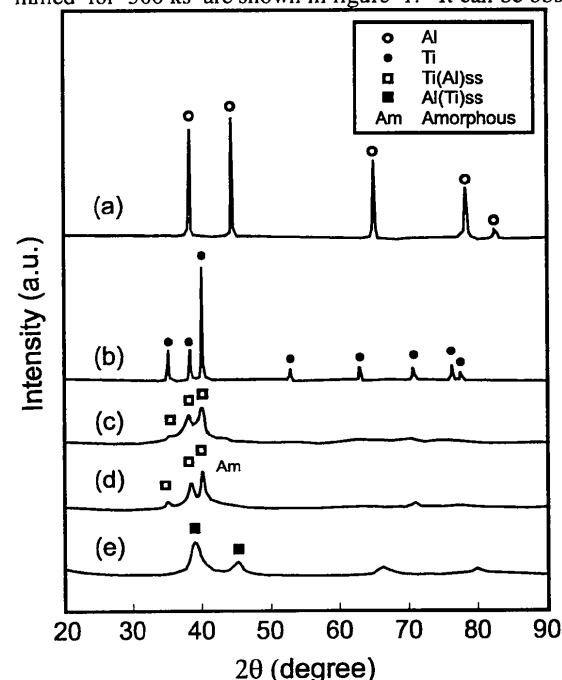


Figure 1
XRD patterns for crystalline Ti (a) and Al (b) powders, $\text{Al}_x\text{Ti}_{1-x}$ milled for 360 ks: $\text{Al}_{0.10}\text{Ti}_{0.90}$ (c), $\text{Al}_{0.50}\text{Ti}_{0.50}$ (d) and $\text{Al}_{0.75}\text{Ti}_{0.25}$ (e).

XRD patterns of $\text{Al}_x\text{Ti}_{1-x}$ alloys are largely different from these of elemental Ti and Al powders due to the solid state reaction produced by the MA. For the $\text{Al}_x\text{Ti}_{1-x}$ samples ($x=0.10$ and 0.50), the typically amorphous diffraction peak appears. Whereas the powders are not perfectly amorphous, a set of small crystalline lines of hcp $\text{Ti}(\text{Al})_{ss}$ solid solution are attached to the broad maximum. The result indicates that a low Al concentration ($x=10$) can drive the $\text{Al}_{0.10}\text{Ti}_{0.90}$ mixture to form amorphous alloy by the MA, and the mixed phases of amorphous state and hcp $\text{Ti}(\text{Al})_{ss}$ solid solution are co-existed in the $\text{Al}_{0.10}\text{Ti}_{0.90}$ and $\text{Al}_{0.50}\text{Ti}_{0.50}$ alloys. However, for the $\text{Al}_{0.75}\text{Ti}_{0.25}$ (aluminum-rich composition) alloy, a completely different behavior can be readily found. The MA leads the $\text{Al}_{0.75}\text{Ti}_{0.25}$ alloy to form only a single phase of fcc $\text{Al}(\text{Ti})_{ss}$ solid solution.

The radial distribution functions (RDF) of $\text{Al}_x\text{Ti}_{1-x}$ samples were obtained from Fourier transformation of the EXAFS function $k^3\chi(k)$. Figure 2 clearly demonstrates that after milling for 360 ks, the intensity of maximum amplitude peak drops about by a factor of two and the peak position contracts about by 0.010, 0.008 and 0.018 nm for $\text{Al}_{0.10}\text{Ti}_{0.90}$, $\text{Al}_{0.50}\text{Ti}_{0.50}$ and $\text{Al}_{0.75}\text{Ti}_{0.25}$ alloys respectively. In particular, we find that there is near the same position and magnitude in the maximum amplitude peak for $\text{Al}_{0.10}\text{Ti}_{0.90}$ and $\text{Al}_{0.50}\text{Ti}_{0.50}$. The result implied that the local structure around Ti atoms in the $\text{Al}_{0.10}\text{Ti}_{0.90}$ is similar that in $\text{Al}_{0.50}\text{Ti}_{0.50}$. However, the position of maximum amplitude peak in $\text{Al}_{0.75}\text{Ti}_{0.25}$ is 0.010 nm shorter than that in $\text{Al}_{0.50}\text{Ti}_{0.50}$. This result suggests that the local structure around Ti atoms produce a large change while the Al atomic concentration x increases from 0.50 to 0.75. The XAFS results are in good agreement with these obtained from XRD.

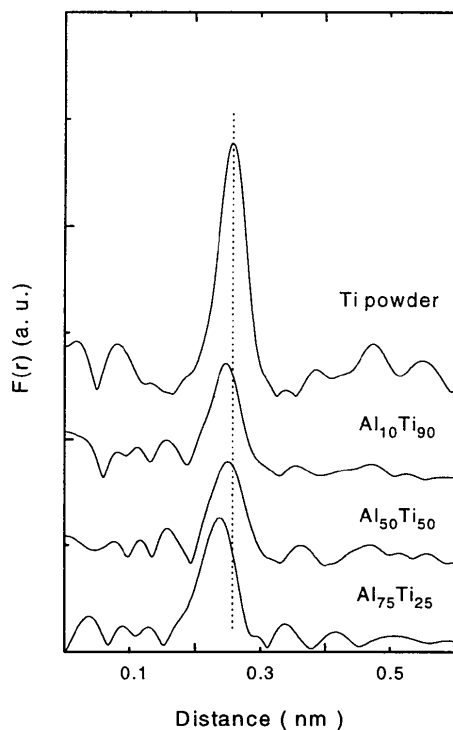


Figure 2
Radial distribution functions of crystalline Ti powder and $\text{Al}_x\text{Ti}_{1-x}$ alloys milled for 360 ks.

For getting structural parameters of nearest neighbor shell of Ti atoms in $\text{Al}_x\text{Ti}_{1-x}$ alloys, the high-frequency noise and the small residual background must be removed. The RDF was inversely transformed to isolate the single shell EXAFS contribution. Using the amplitude $|F(k,p)|$ and phase shift $\delta(k)$ of standard samples obtained from the crystalline Ti powder or FEFF6 (Rehr *et al.*, 1992). The curve fitting results were shown in figure 3. The structural parameters results were summarized in Table 1.

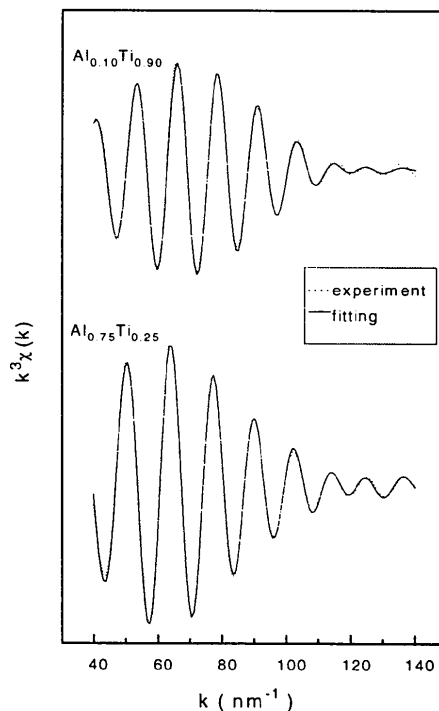


Figure 3
Curve fitting results of $\text{Al}_{0.10}\text{Ti}_{0.90}$ and $\text{Al}_{0.75}\text{Ti}_{0.25}$ alloys milled for 360 ks, using the two coordination subshell (Ti-Ti and Ti-Al).

Table 1
Structural Parameters of $\text{Al}_x\text{Ti}_{1-x}$ alloys milled for 360 ks

sample	pair	$R_i(\text{nm})$	$\sigma_i(\text{nm} \times 10^{-2})$	N
$\text{Al}_{0.10}\text{Ti}_{0.90}$	Ti-Ti	0.296 ± 0.002	1.1 ± 0.10	10.0 ± 1.0
	Ti-Al	0.290 ± 0.002	1.0 ± 0.10	1.0 ± 0.5
$\text{Al}_{0.50}\text{Ti}_{0.50}$	Ti-Ti	0.296 ± 0.002	1.1 ± 0.10	8.5 ± 1.0
	Ti-Al	0.290 ± 0.002	1.0 ± 0.10	2.5 ± 0.5
$\text{Al}_{0.75}\text{Ti}_{0.25}$	Ti-Ti	0.293 ± 0.002	1.0 ± 0.10	5.5 ± 1.0
	Ti-Al	0.286 ± 0.002	1.0 ± 0.10	5.8 ± 1.0

4. Discussions

Schultz (1988) has predicated that the amorphization region of $\text{Al}_x\text{Ti}_{1-x}$ system occurs only in the central composition range about 45-65 atom% Al from thermodynamics viewpoint. His x-ray diffraction patterns have showed that the MA $\text{Al}_{0.48}\text{Ti}_{0.52}$ and $\text{Al}_{0.60}\text{Ti}_{0.40}$ samples become amorphous, but that the MA

$Al_{0.40}Ti_{0.60}$ and $Al_{0.75}Ti_{0.25}$ samples possess crystalline structure. On the contrary, the XAFS and XRD results demonstrate that in the milling condition with a low power the Al_xTi_{1-x} system is preferred to form mixed phases of amorphous state and a partial hcp $Ti(Al)_{ss}$ solid solution for $x=0.10$ and 0.50 . The Al_xTi_{1-x} amorphous alloy range can be greatly extended into a much lower Al concentration ($x=0.10$) which is never reported by previous work. Our MA resultant products influenced by composition are in good agreement with these obtained by Burgio *et al.* (1990) for the Al_xTi_{1-x} system in Ti-rich region.

From table 1, the Ti-Ti and Ti-Al coordination numbers ($N_{Ti-Ti}=8.5$, $N_{Ti-Al}=2.5$) in the $Al_{0.50}Ti_{0.50}$ alloy are significantly deviated from its stoichiometric composition. The Ti atoms favor to be coordinated by Ti atoms for the MA $Al_{0.50}Ti_{0.50}$ alloy. It further indicates that $Al_{0.50}Ti_{0.50}$ powder mixture can not form a uniformly amorphous alloy after ball milling. Moreover, there is a similarly local structure around Ti atoms for both of $Al_{0.10}Ti_{0.90}$ and $Al_{0.50}Ti_{0.50}$ alloys, since their Ti-Ti coordination numbers ($N=10$ and $N=8.5$) are closed. However, for $Al_{0.75}Ti_{0.25}$ alloy, the Ti-Al coordination number abruptly increase to 5.8 and a single phase of fcc $Al(Ti)_{ss}$ solid solution is formed. The results indicates that the formation of Al-Ti amorphous phase depends on the Ti-Ti and Ti-Al coordination number in the first coordination shell of Ti atoms. A small Ti-Al coordination number results in formation of a Al-Ti amorphous phase while a large Ti-Al coordination number produces a $Al(Ti)_{ss}$ solid solution.

The MA mechanism is a complicated process (Cocco *et al.*, 1992). The solid state amorphization by the MA can be attributed to two microscopic origins. One is that the mixed powders are characterized by highly strained small particles with various defects (Ermakov *et al.*, 1981). The other is that a fast diffusion of one element into the host matrix (Dubois *et al.*, 1988). In this work, the radial distribution functions in figure 2 show that there is near the same local neighbor coordination around Ti atoms in both of $Al_{0.10}Ti_{0.90}$ and $Al_{0.50}Ti_{0.50}$ alloys. If all the Al atoms are uniform to be diffused into the Ti host matrix during the MA process, it is difficult to interpret why the local structure around Ti atoms in the MA $Al_{0.10}Ti_{0.90}$ alloy is similar to that in the MA $Al_{0.50}Ti_{0.50}$ alloy. Hence, it seems that the former mechanism is suitable to explain the amorphization mechanism of Al_xTi_{1-x} system by MA in the Ti-rich region. The large deformation of Ti lattice in $Al_{0.10}Ti_{0.90}$ amorphous phase is impossible to be only interpreted as the 10% Al atoms are incorporated into the Ti host matrix by the solid state diffusion. We consider that the amorphization of $Al_{0.10}Ti_{0.90}$ alloy is caused by the Ti lattice defects in which Ti particles were broken down into small grains driven by Al atoms during the MA process. Hellstern and Schultz (1987) have observed that only 8 atom% Zr can lead the $Co_{0.92}Zr_{0.08}$ powder mixture to form amorphous alloy by MA.

In the milling condition with a high power (8 W/g), Gerasimov *et al.* (1996) have found that the Al_xTi_{1-x} resultant products do not depend on the initial state and are determined only by elemental composition. For $Al_{0.30}Ti_{0.70}$ sample, the products were composed of α_2 and bcc phase solid solutions, but not amorphous phase. The structural difference of Al_xTi_{1-x} system obtained by Gerasimov and us can be explained by the effect of excessive heating (Eckert *et al.* 1988), because the local excessive heating is easy to lead the amorphous phase to be crystallized again. Therefore, these results have implied that a metastable Al_xTi_{1-x} amorphous phase can be obtained by controlling a proper milling condition in Ti-rich region.

Our XAFS and XRD results have reveals that in the low milling power a lower Al concentration can only drive Al_xTi_{1-x} mixture to form amorphous phase with the largely defected Ti lattice as Al atoms are interdiffused at the boundary of the Ti grains. However, a higher Al concentration in Al_xTi_{1-x} (in the Al-rich region) is favorable to make most of Al atoms be incorporated into Ti host matrix. Finally, the first nearest neighbor shell of Ti atoms were mainly coordinated by Al atoms and the fcc structural Al_xTi_{1-x} solid solution is formed. why the amorphous phase in the MA Al_xTi_{1-x} alloy can be extended in Ti-rich region (the amorphous state range is extended to 90 atom% Ti), but not in Al-rich region. In fact, it is difficult to propose a good explanation from thermodynamics viewpoint at this moment. The detailed theory and experiment studies need to be worked on the Al_xTi_{1-x} system.

5. Conclusion

XAFS and XRD have been used to measure the local and long range structure information of the MA Al_xTi_{1-x} alloys milled for 360 ks. In the Ti-rich region, the XRD results indicate that the MA with a low power can drive the elemental Al and Ti powders to form mixed phases of amorphous state and hcp $Ti(Al)_{ss}$ solid solution. The Al_xTi_{1-x} amorphous alloy range can be extended to a lower Al concentration ($x=0.10$). The XAFS results further suggest that there are near the same local structures around Ti atoms in both of $Al_{0.10}Ti_{0.90}$ and $Al_{0.50}Ti_{0.50}$ alloys. Ti atoms in $Al_{0.50}Ti_{0.50}$ alloy still favor to be coordinated by Ti atoms. In contrast, the $Al_{0.75}Ti_{0.25}$ alloy possesses a medium-range order, and its Ti atoms are preferable to be coordinated by Al atoms. We found that in the ball milling with a low power, a small Ti-Al coordination number is useful to form a Al-Ti amorphous phase while a large Ti-Al coordination number tend to produce a $Al(Ti)_{ss}$ solid solution.

We would like to thank Beijing Synchrotron Radiation Facility for giving us the beam time for XAFS measurement. This work was partly supported by National Natural Science Foundation of China.

References

- Cocco, G., Enzo, S., Barrett, N.T. & Roberts, Z.J., (1992). *Phys.Rev. B*, **45**, 7066-7076.
- Dubois, J.M., (1988). *J. Less-common Met.*, **145**, 309.
- Eckert, J., Schultz, L., Hellstern, E. & Urban K., (1988). *J.Appl.Phys.*, **64**, 3224.
- Ermakov, A.E., Yivichikov, E.E. & Barinov, V.A., (1981). *Fiz. Met. Metalloved.*, **52**, 1184.
- Fleischer, R.L., Dimiduk, D.M. & Lipsitt, H.A., (1989). *Annu. Rev. Mater. Sci.*, **19**, 231.
- Gerasimov, K.B., Gusev, A.A., Ivanov, E.Y., & Bolderev, V.V., (1991). *J.Mater.Sci.*, **26**, 2459.
- Gerasimov, K.B. & Pavlov, S.V., (1996). *J. of Alloys and Compounds*, **242**, 136-142.
- Hellstern, E. & Schultz, L., (1981). *Philos. Mag. B*, **56**, 443. (1981).
- Kim, Y.W., (1992). *Actametall.*, **40**, 1121.
- Park, Y.H., Hasimoto, H., & Watanabe, R., (1992). *Mater.Sci.Forum.*, **88-90**: 59.
- Rehr, J.J., Zabinsky, S.I., & Albers, R.C., (1992). *Phys. Rev. Lett.* **69**, 3397-3400.
- Sayers, D. E., and Bunker, B. A., (1988). *X-ray Absorption, Principles, Applications, Techniques of EXAFS, SEXAFS and XANES*, p.211-253, edited by Koningsberger, D.C., & Prins, R., John Wiley and Sons, Inc.
- Schultz, L., (1988). *Mater. Sci. Eng.*, **97**, 15-23.
- Wei, S.Q., Oyanagi, H., Wen, C.E., Yang, Y.Z., & Liu, W.H., (1997). *J.Phys.: CM*, **9**, 11077-11083.

(Received 10 August 1998; accepted 21 December 1998)